*American Mineralogist, Volume 84, pages 407–419, 1999*

# Reactions of copper and cadmium ions in aqueous solution with goethite, lepidocrocite, mackinawite, and pyrite

**R.H. PARKMAN,[1,3] J.M. CHARNOCK,[1,2,3] N.D. BRYAN,[3] F.R. LIVENS,[3] AND D.J. VAUGHAN[1,*]**

[1]Department of Earth Sciences (and Geoscience Research Institute), University of Manchester, Manchester M13 9PL, U.K.
[2]CCLRC Daresbury Laboratory, Warrington, Cheshire WA4 4AD, U.K.
[3]Department of Chemistry, University of Manchester, Manchester M13 9PL, U.K.

## ABSTRACT

The uptake of Cu and Cd in aqueous solution by interaction with the surfaces of carefully synthesized finely sized particles of goethite, lepidocrocite, mackinawite, and pyrite was measured as a function of initial metal concentration in solution. The results show how reactions between metal ions in solution and mineral surfaces depend in a subtle way on the nature of the surfaces and, in certain cases, on the initial concentration of metal in solution. The uptake curves fall into two groups; type I in which the efficiency of uptake decreases with increasing concentration (Cu and Cd on goethite and lepidocrocite, Cd on pyrite), and type II in which it remains constant (Cu on mackinawite and pyrite, Cd on mackinawite). The total uptake is an order of magnitude greater for the latter group.

X-ray absorption spectroscopies (XANES and EXAFS) were used to define the local environments of the metals taken up at the mineral surfaces. All examples showing the type I behavior yield information on local environments consistent with their being bound to the surfaces by an inner sphere complex formation mechanism. Thus, Cu on goethite appeared to form a Jahn-Teller distorted octahedral complex (four O atoms at 1.94 Å; two O atoms at 2.41 Å) but with evidence for interaction with two further Fe (or Cu) at 2.92 Å. On lepidocrocite, the first coordination sphere was essentially identical to that on goethite but with a second Cu or Fe shell at 3.04 Å and, for the highest Cu loadings, a third shell (2 Cu or Fe) at 3.67 Å. The Cd on goethite showed best fits for sixfold coordination to O (at 2.26 Å) but with evidence for a second shell of Fe atoms at 3.75 Å. On lepidocrocite, the first shell was essentially the same as for goethite, but a second shell of Fe atoms appeared to occur at the shorter distance of 3.31 Å. For Cd-loaded pyrite, best fits were given by a single shell of six O atoms at 2.27 to 2.28 Å and with no evidence for a second shell of metal atoms. The systems exhibiting the type II behavior yielded spectra consistent with the formation of new phases on the surfaces, either by precipitation or replacement reactions. In the case of Cu interaction with mackinawite, a chalcopyrite phase appeared to form, whereas interaction with pyrite seemed to produce binary Cu sulfides—covellite at lower loadings and chalcocite at higher loadings. Cd interaction with mackinawite seemed to produce a CdS phase.

## INTRODUCTION

Surface interactions of Fe minerals are of interest because of their importance in Recent sediments in many estuaries and near-shore marine areas. For example, Fe oxyhydroxides occur as components of muds in the oxidizing environment at or near the surface and in the reducing environment just beneath the surface, Fe monosulfides occur and transform to pyrite during diagenesis. These phases are very fine particle materials that present large surface areas for interaction with species in the solutions in contact with them. Their surface chemistries are of particular interest and as is the chemistry associated with this critically important ''redox boundary'' (DiToro et al. 1996). Although several Fe oxyhydroxide and sulfide phases occur in sediments, goethite is the most important of the oxyhydroxides, and mackinawite is the predominant, initially formed, Fe sulfide. Also, the first formed Fe sulfide in aqueous systems, even though it is X-ray amorphous, has the local structure of mackinawite (Lennie and Vaughan 1996). Copper pertains because it represents wastes derived from metalliferous mining. This transition metal also has an interesting redox chemistry. Cadmium also occurs in mine wastes and as a waste from various industrial activities; this heavy metal is toxic to humans and many other biota.

Previously interactions between Cu and goethite were studied using bulk measurements of adsorption (Forbes et al. 1976; Balistrieri and Murray 1982; Padmanabham

* E-mail: david.vaughan@man.ac.uk

0003–004X/99/0003–0407$05.00

1983; Kooner 1992, 1993). These studies indicated significant uptake was dependent on goethite surface area but insensitive to variations in ionic strength of the medium. At higher pH values, hydrolysis occurred and up to two protons were released per $Cu^{2+}$ taken up. To our knowledge, only one study of the reactions of Cu at the water-goethite interface was undertaken using XAS (Bochatay et al. 1997). In accord with models based on bulk measurements, this study pointed to the formation of inner sphere Cu complexes at the goethite surface. Although only O atoms at ~1.94 Å could be identified in the first coordination shell surrounding Cu, these could represent the four equatorial O atoms of a Jahn-Teller distorted octahedral complex. Evidence existed for a second shell of metal atoms at 2.96 Å, attributed to Cu atoms associated with hydroxo-bridged $Cu^{2+}$ surface polymers. For Cd interaction with Fe oxyhydroxide surfaces, studies involved both bulk measurements (Forbes et al. 1976; Benjamin and Leckie 1981; Dzombak and Morel 1990) and XAS experiments (Spadini et al. 1994). The bulk measurements point to surface sorption reactions, and the stoichiometry and thermodynamic stability of the relevant surface complexes were deduced from sorption experiments. Equilibrium constants for Cd sorbed on hydrous ferric oxides decreased with increased surface loading, suggesting that various surface sites were involved. XAS studies suggested that at low surface coverage Cd atoms mainly sorb at the termination of α-FeOOH chains on (001) planes by sharing edges and corners with surface Fe octahedra. At medium and high-surface loading, Cd atoms sorbed along chains on (*hk*0) planes where they shared mainly corners with Fe octahedra.

Several studies aimed to elucidate interactions between Cu or Cd in solution and the surfaces of Fe monosulfides (Watson et al. 1994; Watson and Ellwood 1994; Morse and Arakaki 1993). Only Morse and Arakaki (1993) specifically identified the substrate as mackinawite, but their work involved only bulk measurements, not XAS. These studies showed that FeS has excellent sorptive properties with respect to a range of metals, including Cu and Cd, consistent with the observations of natural sediments (DiToro et al. 1996). Bulk measurements were made of the interaction of Cd (and other divalent cations) with the surface of pyrite by Kornicker and Morse (1991) and interpreted using an ionic exchange surface complex formation model. The observed behavior suggested more complex adsorption.

To investigate the various possible interactions between metal ions in aqueous solution and the surfaces of common minerals, experimental studies of the interaction of Cu and Cd ions and the surfaces of goethite (α-FeOOH), lepidocrocite (γ-FeOOH), mackinawite (FeS), and pyrite ($FeS_2$) were undertaken. Here, carefully synthesized and characterized powdered samples of goethite, lepidocrocite, mackinawite, and pyrite were exposed (in batch experiments) to aqueous solutions containing varying concentrations of Cu and Cd ions, and the uptake of metal from solution measured as a function of initial concentration. The form in which the metal had been taken up by the mineral was then investigated using X-ray absorption spectroscopy (XAS). We focused particularly on comparisons between the oxide and sulfide substrates and between the two metals.

## METHODS

### Synthesis of mineral substrates

Goethite and lepidocrocite were prepared using the methods described by Schwertmann and Cornell (1991). For goethite synthesis, ferrihydrite was initially precipitated by adding 180 mL of 5 *M* KOH (freshly prepared) to 100 mL of a 1 *M* aqueous solution of $FeCl_3 \cdot 6H_2O$ in a 2 L polythene beaker. The resulting suspension was vigorously stirred and diluted to 2 L with deionized water. The beaker was covered and held at 70 °C for 60 h to convert the ferrihydrite precipitate to goethite. The precipitate was centrifuged, washed several times with deionized water, and freeze-dried. The purity and homogeneity of the goethite sample was confirmed by powder X-ray diffraction (XRD). Goethite synthesized by this method typically has a surface area of 20 $m^2/g$. Morphological and spectroscopic data were included in Schwertmann and Cornell (1991).

Lepidocrocite was prepared by oxidation of $Fe^{2+}$ in aqueous solution at controlled pH. A solution of unoxidized $FeCl_2 \cdot 4H_2O$ (300 mL, 0.2 *M* in degassed $H_2O$) was filtered, then adjusted to pH 6.7 to 6.9 with freshly prepared 1 *M* NaOH solution. $CO_2$-free air was bubbled through the solution, with constant stirring, and the pH was adjusted with 1 *M* NaOH during reaction to maintain it in the range 6.5 to 7.0. After reaction was complete, the lepidocrocite precipitate was centrifuged, washed several times with deionized water, and freeze-dried. The mineralogical identity of the product was confirmed by powder XRD. The surface area of lepidocrocite synthesized in this way was generally 70 to 80 $m^2/g$, and the morphology was described in Schwertmann and Cornell (1991).

Synthesis of mackinawite (tetragonal FeS) was based on the procedure used by Lennie and Vaughan (1996). A ball of Fe wire was suspended in a 0.5 *M* $CH_3CO_2Na/CH_3CO_2H$ buffer (500 mL; pH 4). Partial dissolution of the Fe wire by reaction with the acetate buffer (~2 h) evolved $H_2$ gas and provided a reducing environment. Separate solutions of $FeSO_4 \cdot 7H_2O$, then $Na_2S \cdot 12H_2O$ (each 60 mL, 0.1 *M),* previously prepared using de-aerated deionized water, were added to the reaction vessel, and a thick black suspension immediately resulted. The precipitate was filtered and washed with de-aerated deionized water before being freeze-dried. The resulting fine black powder was then stored in a nitrogen atmosphere until it was needed for the experiments (although to reduce the storage time, separate batches of FeS were prepared for the Cu and Cd experiments). Both of these samples were amorphous when examined by X-ray powder diffraction, but EXAFS analysis of the Fe K-edge

gave coordination numbers and interatomic distances (4 S atoms at 2.20 Å and 4 Fe atoms at 2.5 to 2.6 Å) consistent with Lennie et al. (1995) and Lennie and Vaughan (1996) and confirmed their mineralogical purity. It is not possible to make a sensible estimate of the surface area of this material, because it is very prone to oxidation and other investigators (Watson et al. 1994) have found that different methods yield results differing by more than two orders of magnitude.

Pyrite was synthesized by heating high purity Fe and S powders in evacuated, sealed silica capsules (Vaughan and Craig 1978). The reaction product was checked by XRD and confirmed to be pure pyrite. No estimate of surface area is available.

**Batch experiments**

The experiments were conducted in 50 mL capped polyethylene centrifuge tubes using a solid/solution ratio of 0.1 g/10 mL. For the Cu-goethite and Cu-lepidocrocite experiments, samples of the solid material were contacted overnight with deionized water (9.9 mL) before adding a 100 μL aliquot of aqueous $Cu(NO_3)_2$ of compositions to give initial solution concentrations of between 0.0 and 3.0 m*M*. Four replicate experiments were conducted for each concentration (one for pH measurement) and a contact time of 24 h was used. No constraints were imposed on pH during the course of these reactions, but the final pH value was recorded. The samples used for Cu analysis were centrifuged at 10 000 rpm for 1 h. An aliquot of known volume was taken from the supernatant liquid and diluted (at least 100×) with 2% (v/v) $HNO_3$ (Analar). All samples were analyzed by Inductively Coupled Plasma Mass Spectrometry (ICPMS) in Pulse Counting mode (working range about <50 ppb), using $^{115}In$ as an internal standard. Appropriate reagent and experimental blanks were analyzed throughout and found to contain negligible (<5% of that arising from the added Cu) amounts of Cu. At the end of the analysis, the concentration of Cu remaining in solution was determined and the amount of Cu taken up calculated by difference. Essentially the same procedure was used for the Cd-goethite and Cd-lepidocrocite experiments, except that the Cd was introduced as an aqueous solution of $CdSO_4$.

For the mackinawite and pyrite experiments, all sample manipulations were carried out in a nitrogen atmosphere. Samples of the solid material (100 mg) were contacted overnight with degassed, deionized water (9.9 mL) before adding a 100 μL aliquot of aqueous $Cu(NO_3)_2$ of compositions to give initial solution concentrations between 0.0 and 5.0 m*M*. Three replicate experiments were conducted for each concentration and a contact time of 24 h was used. The samples used for Cu analysis were centrifuged at 10 000 rpm for 1 h, then the supernatant was withdrawn and filtered through a 0.45 μm filter. An aliquot of known volume was taken from the supernatant and allowed to reoxidize, in the course of which hydrated Fe oxides precipitated. These were dissolved again by the addition of a known volume of 10% (v/v)$HNO_3$, then the solution was diluted and analyzed by Inductively Coupled Plasma Mass Spectrometry (ICPMS) in Pulse Counting mode (working range about <50 ppb) using $^{115}In$ as an internal standard. The results were calculated as previously described.

**X-ray absorption spectroscopy (XAS)**

Cu and Cd K-edge absorption spectra were collected for representative samples of goethite, lepidocrocite, mackinawite, and pyrite, which had been exposed to Cu and Cd in solution. Samples for XAS were prepared as for the batch experiments, except that a larger quantity of material was used (0.3 g/30 mL) to provide enough solid material for spectroscopic analysis. The initial Cu and Cd concentrations were chosen after studying the results of the batch experiments for the four mineral phases (Fig. 1). The concentrations of Cu and Cd taken up by these samples were similar to the quantities taken up in the batch experiments. In addition to the above samples, Fe, Cu, and Cd K-edge X-ray spectra were recorded for the unreacted goethite, lepidocrocite, mackinawite, and pyrite powders (as ''blanks'') and Cu and Cd K-edge spectra for 50 m*M* aqueous solutions were also collected.

All of the spectra were collected at the CLRC Daresbury Laboratory Synchrotron Radiation Source (SRS). The Cu and Fe K-edge spectra (at energies of 8979 and 7112 eV respectively) were collected on Station 8.1 and the Cd K-edge spectra (at 26711 eV) were collected on Station 9.2. Appropriate metal foils were used for energy calibration. Typical beam conditions were 150 mA current, 2 GeV energy. The Cu and Cd loaded mineral samples were analyzed as slurries at liquid nitrogen temperature using an evacuated cryostat and were enclosed in cells with impermeable windows to prevent freeze drying. Measurements at room temperature showed that the freezing procedure, which improved spectral quality, did not alter the results (Farquhar et al. 1997). The ''blanks'' and solutions were analyzed at room temperature. All of the spectra were measured in fluorescence mode using a Canberra 13 element solid state detector, except the spectra for the solutions and the Fe K-edge spectra for the mackinawite, which were measured in transmission mode. A Si(220) double crystal monochromator was used and detuned to reject 50% of the signal to minimize harmonic contamination. Multiple scans (up to 10) were used to improve the signal to noise ratios for samples with low metal concentrations.

After the spectra had been collected, the SRS Daresbury Laboratory programs EXCALIB and EXBACK were used to manipulate the data. The isolated extended X-ray absorption fine structure data (EXAFS) obtained from these programs were then analyzed using the EXCURV92 (Binsted et al. 1991) and EXCURV97 programs. These programs utilize the spherical wave approximation (Lee and Pendry 1975; Gurman et al. 1984). Phaseshifts were derived in the program from ab initio calculations using Hedin-Lundqvist potentials (Hedin and Lundqvist 1969) and Von Bart ground states. A Fourier

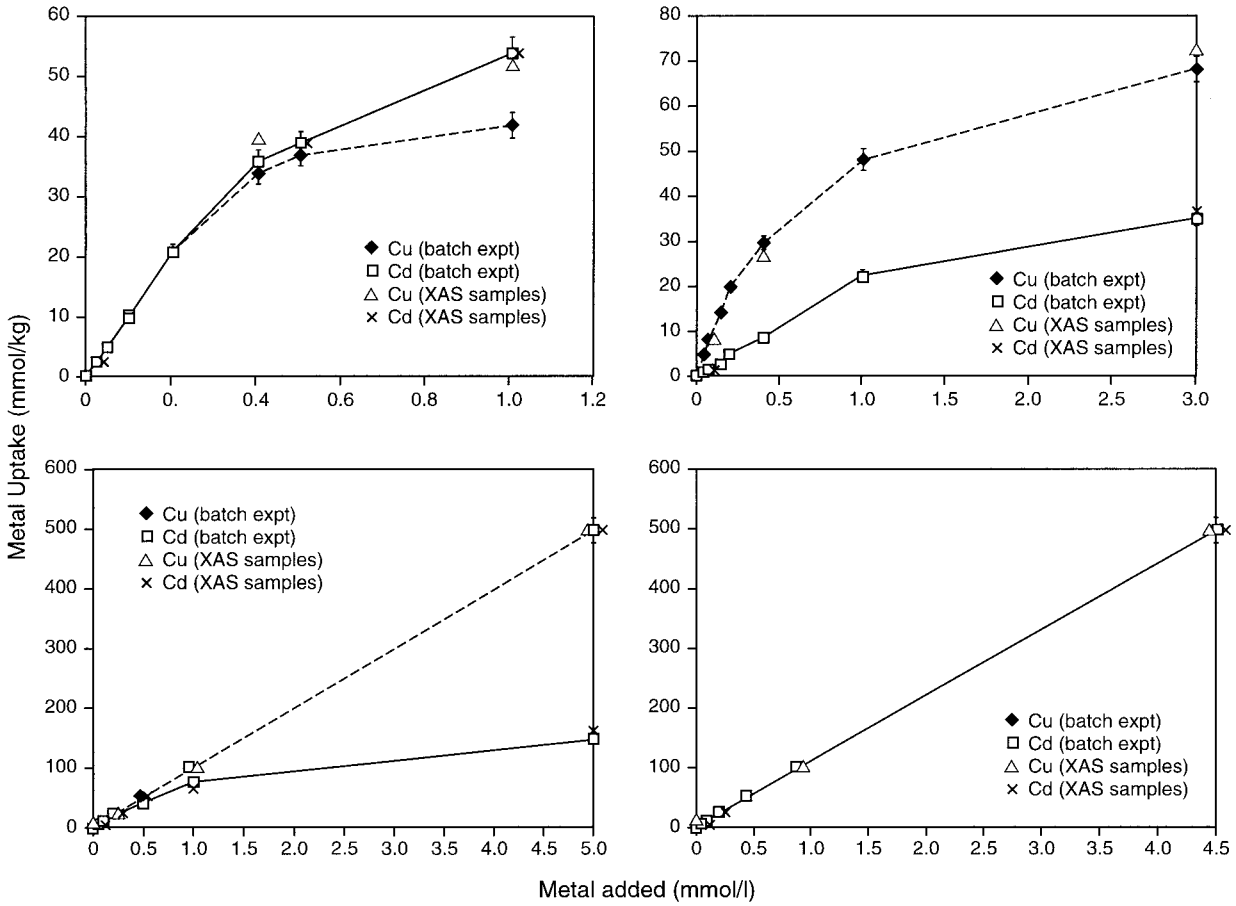


**FIGURE 1.** Uptake of $Cu^{2+}$ and $Cd^{2+}$ on goethite, lepidocrocite, mackinawite, and pyrite. Solid lines represent $Cd^{2+}$ uptake; broken lines represent $Cu^{2+}$ uptake. Each point represents the mean of three replicates, error bars are ±1 standard deviation.

transform of the experimental spectrum provides an approximate radial distribution function around the central absorbing atom (i.e., Cu or Cd). The peaks in the Fourier transform represent ''shells'' of atoms surrounding the central Cu or Cd. These are used to develop a model of the coordination site of the Cu or Cd from which a theoretical spectrum is calculated. The closeness of fit between the theoretical spectrum and the experimental spectrum is measured by a least squares residual (R). The smaller the value of this parameter, referred to here as the ''R-factor'', the better the fit between the experimental and theoretical spectrum. An initial fit for each shell of atoms is obtained by changing the number, *N*, and type of backscatterers (ligands) that surround the central absorber (Cu or Cd). Once this is achieved, the Debye-Waller factor, $2\sigma^2(Å^2)$, and the distance, $r(Å)$, are iteratively adjusted, together with a third parameter, the Fermi energy, $E_f$, to produce the best fit. Further shells may be added to improve the model and can be tested statistically using the significance tests of Joyner et al. (1987). This process is repeated by varying coordination numbers and ligand types until the best fit is achieved but, in this work, only those shells that improved the fit at the 1% significance level were accepted. A range of model compounds of known structure was also analyzed and the coordination numbers and interatomic distances determined by fitting these spectra were within error of those determined crystallographically.

### Thermodynamic modeling

The geochemical modeling code PHREEQE 96 (Arthur and Tyrer 1996), together with the CHEMVAL6 database, was used to provide an insight into the outcome of the batch uptake experiments. The solubilities of all the solid phases used are low with mackinawite giving predicted dissolved Fe concentrations of the order of $10^{-6}$ *M* and the other phases giving much smaller concentrations, in the range $10^{-9}$ to $10^{-14}$ *M*. The pH values used in the calculations were set at the experimental values and the speciation of 1 m*M* (for the oxyhydroxides) and 3 m*M* (for the sulfides) $Cu^{2+}$ and $Cd^{2+}$, equilibrated with the appropriate mineral phase, was calculated.

## RESULTS

### Batch experiments

Details of the batch uptake experiments are given in Tables 1 and 2. Results of these experiments are illus-

**TABLE 1.** Initial solution concentrations, quantities and percentages taken up, final pH values for batch experiments involving Cu and Cd solution species and the goethite and lepidocrocite substrates

| Initial solution conc | | | Quantity taken up | | | |
|---|---|---|---|---|---|---|
| m*M* | ppm | Final pH | mmol/kg | ppm on solid phase | % uptake | % precision (RSD) |
| | | | **Cu on goethite** | | | |
| 0.000 | 0 | 7.9 | | | | |
| 0.025 | 1.6 | 7.9 | 2.50 | 159 | 99.8 | 0.8 |
| 0.050 | 3.2 | 7.9 | 4.82 | 306 | 99.6 | 1.1 |
| 0.100 | 6.4 | 7.7 | 10.3 | 654 | 98.5 | 0.3 |
| 0.200 | 12.8 | 7.4 | 20.6 | 1310 | 98.3 | 1.0 |
| 0.400 | 25.6 | 5.3 | 33.4 (39.0) | 2120 (2480) | 81.1 (97.2) | 0.4 |
| 0.500 | 32.0 | 5.0 | 35.6 | 2260 | 70.6 | 1.3 |
| 1.000 | 64.0 | 4.7 | 41.9 (53.6) | 2660 (3400) | 41.9 (50.3) | 1.3 |
| | | | **Cd on goethite** | | | |
| 0.000 | 0 | 7.7 | | | | |
| 0.025 | 2.8 | 7.7 | 2.48 (2.04) | 283 (233) | 99.4 | 1.5 |
| 0.100 | 11.3 | 7.6 | 9.99 | 1140 | 99.9 | 1.2 |
| 0.200 | 22.4 | 7.4 | 19.9 | 2280 | 99.5 | 1.0 |
| 0.400 | 45.4 | 5.8 | 35.0 (35.1) | 3980 (4000) | 87.6 (97.2) | 0.8 |
| 0.500 | 56.5 | 5.4 | 39.3 | 4480 | 78.6 | 1.8 |
| 1.000 | 113.5 | 5.1 | 53.3 (53.6) | 6080 (6100) | 53.5 (53.8) | 0.9 |
| | | | **Cu on lepidocrocite** | | | |
| 0.000 | 0 | 7.8 | | | | |
| 0.050 | 3.1 | 7.8 | 4.56 | 287 | 91.2 | 1.3 |
| 0.075 | 4.7 | 7.8 | 7.40 (8.00) | 468 (506) | 98.7 (106.7) | 1.1 |
| 0.150 | 9.4 | 7.6 | 14.0 | 886 | 93.3 | 1.1 |
| 0.200 | 12.8 | 7.4 | 19.5 | 1230 | 97.5 | 0.7 |
| 0.400 | 25.6 | 5.7 | 29.5 (27.0) | 1870 (2270) | 73.8 (67.5) | 0.6 |
| 1.000 | 64.0 | 5.5 | 48.0 | 3040 | 48.0 | 0.8 |
| 3.000 | 192.0 | 4.9 | 68.0 (72.0) | 4300 (4550) | 22.7 (24.0) | 1.0 |
| | | | **Cd on lepidocrocite** | | | |
| 0.000 | 0 | 7.8 | | | | |
| 0.050 | 5.6 | 7.8 | 0.90 | 101 | 60.0 | 1.1 |
| 0.075 | 8.5 | 7.8 | 1.20 (1.20) | 134 (134) | 53.3 (53.3) | 1.0 |
| 0.150 | 17.0 | 7.7 | 2.40 | 269 | 53.3 | 1.8 |
| 0.200 | 22.7 | 7.42 | 4.80 | 538 | 80.0 | 1.0 |
| 0.400 | 45.4 | 5.8 | 8.40 (8.00) | 941 (896) | 70.0 (66.7) | 1.4 |
| 1.000 | 113.5 | 5.5 | 22.2 | 2490 | 74.0 | 1.2 |
| 3.000 | 340.5 | 4.8 | 34.7 (36.0) | 3890 (4030) | 38.6 (40.0) | 0.6 |

*Notes:* Values in parentheses are for the equivalent samples prepared for XAS measurement; all uptake data are the mean of three replicate measurements.

trated in Figure 1. Similar information is also presented for the separate, larger samples prepared for XAS analysis.

In some cases, uptake on the XAS samples was outside the range expected from the batch experiments, suggesting that variability between experiments was greater than that within experiments. Although the efficiency of metal uptake varied, depending on the element and solid phase used, the final pH in the oxyhydroxide experiments was close to that found when the solid phase reacted with water, up to an initial metal concentration in solution of approximately 0.2 m*M*. This suggests that the pH of the oxyhydroxide systems was buffered, probably by exchange of protons with the surface. Beyond a metal concentration of 0.2 m*M* in the oxyhydroxide experiments, the pH started to fall, suggesting the buffer capacity of the systems was exceeded. The pH rose on reaction of mackinawite with water, reflecting dissolution of the solid mackinawite, and the pH remained essentially unchanged even with the highest metal additions. Pyrite, being much less soluble than mackinawite, caused only a small increase in pH but still appeared to be pH-buffered.

## Geochemical modeling

For the goethite and lepidocrocite experiments, the thermodynamic calculations indicated that the stable Fe phase is hematite, although no experimental evidence for the transformation of lepidocrocite or goethite to hematite was found. For Cu experiments, the system was supersaturated with respect to $Cu(OH)_2$ although precipitation, which is observable, was not actually observed on addition of the Cu spike. For the Cd experiments, the system was undersaturated with respect to all plausible solid phases. Little change of pH was expected on equilibration of the oxyhydroxides with water due to their low solubilities, and little change was actually observed.

For the sulfide experiments, the solubility of the solid phases was low (about $5 \times 10^{-7}$ *M*), and only $10^{-3}$% of the total dissolved sulfide species was expected to be present as $S^{2-}$ at the experimental pH values, so that the

**TABLE 2.** Initial solution concentrations, quantities and percentages taken up, final pH values for batch experiments involving Cu and Cd solution species and the mackinawite and pyrite substrates

| Initial solution conc. | | Final | Quantity taken up | | | |
|---|---|---|---|---|---|---|
| m*M* | ppm | pH | mmol/kg | ppm on solid phase | % uptake | % precision (RSD) |
| | | | **Cu on mackinawite** | | | |
| 0.000 | 0 | 7.1 | | | | |
| 0.050 | 3.2 | 7.0 | 4.98 | 314 | 99.6 | 1.5 |
| 0.100 | 6.4 | 6.9 | 9.97 | 628 | 99.7 | 1.3 |
| 0.250 | 15.8 | 6.8 | 25.2 | 1580 | 100.8 | 1.1 |
| 0.500 | 31.6 | 6.8 | 49.7 (49.4) | 3130 (3110) | 99.4 (98.8) | 1.7 |
| 1.000 | 63.2 | 6.9 | 99.8 (104) | 6290 (6550) | 99.8 (104.0) | 0.8 |
| 5.000 | 316.0 | 6.7 | 503 (495) | 31700 (31200) | 100.6 (99.0) | 1.1 |
| | | | **Cd on mackinawite** | | | |
| 0.000 | 0 | 7.2 | | | | |
| 0.050 | 5.7 | 7.2 | 5.01 (5.04) | 565 (568) | 100.2 (100.8) | 1.8 |
| 0.100 | 11.3 | 7.1 | 9.99 | 1140 | 99.9 | 0.8 |
| 0.250 | 28.2 | 6.9 | 24.7 | 2810 | 98.8 | 1.3 |
| 0.500 | 56.4 | 6.9 | 49.9 (50.5) | 5680 (5750) | 99.8 (101.0) | 1.4 |
| 1.000 | 112.8 | 6.7 | 100.3 | 11400 | 100.3 | 1.7 |
| 5.000 | 564.0 | 6.7 | 497.8 (504.6) | 56600 (57400) | 99.6 (100.9) | 1.2 |
| | | | **Cu on pyrite** | | | |
| 0.000 | 0 | 7.2 | | | | |
| 0.050 | 3.2 | 7.2 | 5.16 | 325 | 103.2 | 1.4 |
| 0.100 | 6.4 | 7.1 | 9.89 (10.3) | 623 (649) | 98.9 (100.3) | 1.1 |
| 0.250 | 15.8 | 7.1 | 25.5 (24.5) | 1670 (1600) | 102.0 (98.0) | 1.1 |
| 0.500 | 31.6 | 7.0 | 49.6 | 3250 | 99.2 | 1.4 |
| 1.000 | 63.2 | 6.9 | 102.5 (102.7) | 6720 (6740) | 102.5 (102.7) | 1.6 |
| 5.000 | 316.0 | 6.9 | 507.8 (503.0) | 33300 (32900) | 101.6 (100.6) | 0.9 |
| | | | **Cd on pyrite** | | | |
| 0.000 | 0 | 7.1 | | | | |
| 0.050 | 5.7 | 7.2 | 4.90 | 554 | 98.0 | 0.6 |
| 0.100 | 11.3 | 7.1 | 10.2 (9.80) | 1150 (1100) | 102.0 (98.0) | 1.4 |
| 0.250 | 28.2 | 7.0 | 22.4 (24.0) | 2530 (2710) | 89.6 (96.0) | 0.9 |
| 0.500 | 56.4 | 7.0 | 40.8 | 4610 | 81.6 | 1.2 |
| 1.000 | 112.8 | 7.1 | 77.8 (80.0) | 8790 (9040) | 77.8 (80.0) | 0.8 |
| 5.000 | 564.0 | 6.8 | 143.2 (155.1) | 16200 (17500) | 28.7 (31.0) | 1.0 |

*Notes:* Values in parentheses are for the equivalent samples prepared for XAS measurement; all uptake data are the mean of three replicate measurements.

systems were predicted to be undersaturated with respect to sulfide phase precipitation. Particularly in the case of mackinawite, the calculated equilibrium pH was higher than the pH actually observed. All the sulfide experiments appeared to be pH buffered, although there was a slight drop in pH as metal loading increased. The Cu experiments were actually predicted to be supersaturated with respect to $Cu(OH)_2$ and the Cd experiments to be undersaturated with respect to any solid phase.

### X-ray absorption spectroscopy

Initial metal concentrations for preparation of samples for XAS analysis were selected from the ranges used in the batch experiments. Partitioning between solid phase and solution was measured for these samples and the results are plotted in Figure 1. The extent of uptake by the XAS samples was generally similar to that observed in the batch experiments.

**Cu on oxides.** The X-ray absorption near edge structure (XANES) can be used qualitatively to characterize the local environment of the metal. The Cu K-edge XANES for Cu in the original solution, sorbed to the mineral phases studied here and in related compounds, are shown in Figure 2. The XANES of Cu on both oxides was very similar to that of $[Cu(H_2O)_6]^{2+}$, suggesting a local environment in which Cu was coordinated to O in an approximately octahedral geometry. The sulfide phases are discussed below.

Examples of the Cu K-edge EXAFS for Cu on goethite and lepidocrocite, together with the associated Fourier transforms, are shown in Figures 3 and 4. The best fits for Cu on both oxide surfaces were found with sixfold coordination to O in a Jahn-Teller distorted environment with four close O atoms (1.94 Å on goethite, 1.96 Å on lepidocrocite) and two more distant O atoms (at 2.41 Å on goethite, 2.43 Å on lepidocrocite) completing the first coordination sphere. On goethite, a second shell of cations at 2.92 Å was also found. These two further cations could be either Cu or Fe, whose backscattering properties were too similar to allow their distinction. On lepidocrocite, the second cation shell was at a distance of ~3.04 Å, and at the highest Cu loading, a third shell of two further cations at 3.67 Å was also identified.

**Cu on sulfides.** The XANES data for Cu on mackinawite (Fig. 2) dramatically differed from those for the solution species, $[Cu(H_2O)_6]^{2+}$, for Cu on Fe oxide surfaces, and for the simple binary sulfides covellite and chalcocite, but they closely resembled the spectrum ob-

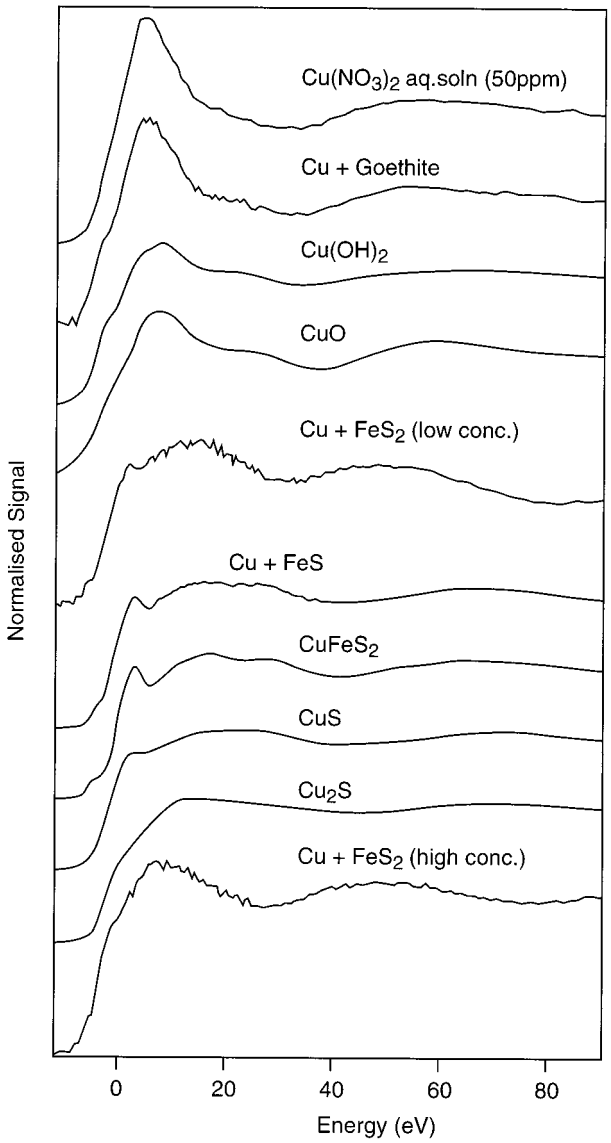


**FIGURE 2.** Cu K-edge XANES for model species and Cu-loaded Fe oxides and sulfides.

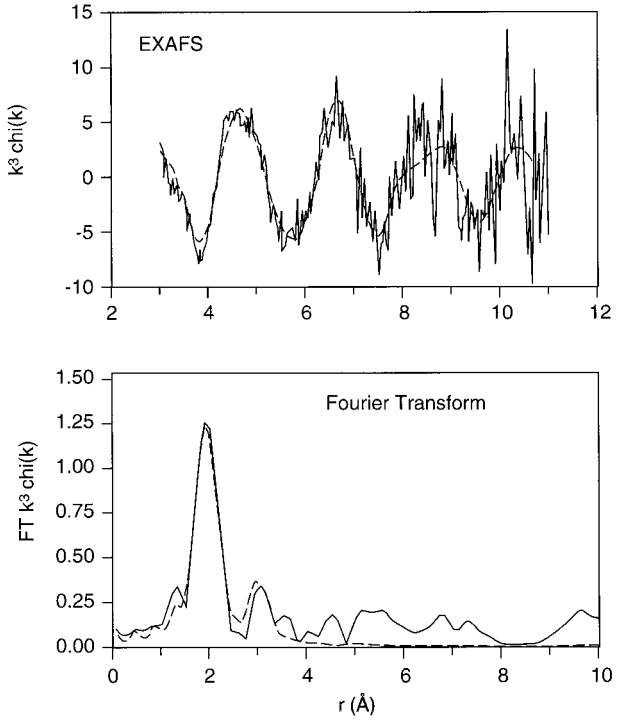


**FIGURE 3.** EXAFS and Fourier transforms for $Cu^{2+}$ on goethite (initial solution concentration 1.0 mmol/L; Cu loading 53.6 mmol/kg).

tained for the ternary sulfide mineral chalcopyrite. At the lowest loading, the XANES for Cu on pyrite resembles that of covellite and at the highest loading resembles that of chalcocite. The XANES spectra at intermediate loadings appear to be transitional between the two phases identified above. In both cases, therefore, XANES suggested that reaction of Cu with the sulfide surfaces led to formation of one or more distinct mineral phases.

The EXAFS data for Cu on mackinawite (Fig. 5) were consistent with the XANES. The best fits showed fourfold-coordinate Cu atoms with sulfur at 2.29 Å and further Cu or Fe atoms at 3.74 Å, as expected for a chalcopyrite-type phase (Parkman et al. 1996). EXAFS analysis of Cu on pyrite (Fig. 6) at all loadings generally showed similar results. Cu is in fourfold-coordination with S atoms at 2.30 Å, and a second shell of 2 Fe or Cu atoms is present at 3.80 Å, consistent with the formation of one of several binary Cu-sulfide phases. The structural similarity of the various candidate phases meant that the phase or phases formed could not be identified unambiguously from the EXAFS alone.

**Cd on oxides.** The Cd K-edge XANES of Cd on goethite and lepidocrocite (Fig. 7) closely resembled the spectrum for $Cd(OH)_2$ or $[Cd(H_2O)_6]^{2+}$. The EXAFS spectra and associated Fourier transforms for Cd on goethite (Fig. 8) showed best fits for Cd in sixfold coordination to O at a distance of 2.26 Å. A significant improvement in fit was achieved by adding a second shell of Fe (rather than Cd) atoms at a distance of 3.75 Å. The results for the goethite samples with other Cd loadings were not substantially different, except that the best fit numbers of Fe atoms in the second shell varied somewhat, between 1 and 3. In the case of lepidocrocite (Fig. 9), the best fit was again achieved with a first shell of 6 O atoms at ~2.28Å, within error of the distance found for the goethite samples. There was again evidence for a second shell composed of Fe atoms, although the distances were 3.31 Å, less than those found in the goethite samples. Best fit numbers of Fe atoms in this second shell varied between 2 and 3. At all three Cd loadings, the fit was improved by the inclusion of a third Fe shell (1 Fe at 3.77 Å), although the improvement was only significant at the 1% level in the sample with the highest Cd loading.

**Cd on sulfides.** The Cd K-edge XANES spectrum for

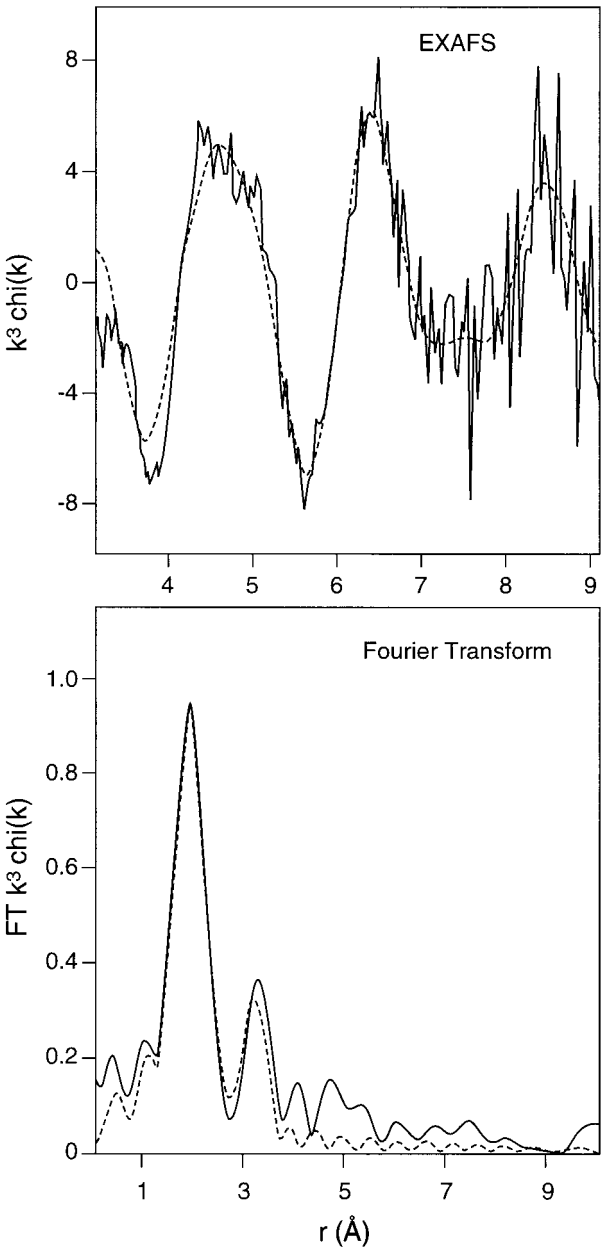


**FIGURE 4.** EXAFS and Fourier transforms for $Cu^{2+}$ on lepidocrocite (initial solution concentration 3.0 mmol/L; Cu loading 72.0 mmol/kg).

Cd on FeS differed from that for Cd in solution and most closely resembled that for solid CdS (Fig. 7). Because of the low concentration of Cd taken up by the pyrite surface, the quality of the XANES spectrum was poor. However, the spectral profile clearly resembled that for Cd bonded to O and not Cd bonded to S. This observation suggests a fundamental difference in the interactions of Cd with the two sulfide surfaces.

For mackinawite, the XANES evidence for formation of a Cd-S phase was supported by the Cd K-edge EXAFS spectra and their Fourier transforms (Fig. 10), which showed a single shell of four S atoms at 2.52 Å, extremely close to the Cd-S distance in hawleyite. There was no evidence of a second coordination shell, perhaps because this surface CdS phase was poorly ordered.

At all Cd loadings, EXAFS analysis of Cd-loaded pyrite gave a best fit with a single shell of six O atoms at 2.27–2.28 Å (Fig. 11), very similar to the first shell data obtained from the Cd-loaded oxides. There was no evidence for a second shell of metal atoms. In all cases, attempts to model the spectra with S atoms, rather than O, gave substantially poorer fits to the data and also led to unreasonably short Cd-S distances (2.4 Å as opposed to the more normal 2.5 Å). These analyses, together with the XANES, strongly suggest that Cd remains coordinated by O atoms on reaction with the pyrite surface in contrast to its interaction with mackinawite.

**TABLE 3.** Summary of EXAFS data fitting for Cu

| Sample | CN and type | $r$ (Å) | $2\sigma^2$ (Å$^2$) | $R$ |
|---|---|---|---|---|
| Goethite | 4 O | 1.94 | 0.009 | 51.4 |
| | 2 O | 2.41 | 0.023 | |
| | 2 Cu or Fe | 2.92 | 0.020 | |
| Lepidocrocite | 4 O | 1.96 | 0.009 | 43.6 |
| | 2 O | 2.43 | 0.038 | |
| | 2 Cu or Fe | 3.04 | 0.021 | |
| | 2 Cu or Fe | 3.67 | 0.018 | |
| Mackinawite | 4 S | 2.29 | 0.012 | 31.1 |
| | 4 Cu or Fe | 3.74 | 0.026 | |
| Pyrite | 4 S | 2.30 | 0.017 | 33.6 |
| | 2 Cu or Fe | 3.80 | 0.021 | |

*Notes:* CN is coordination number, $r$ is interatomic distance, $2\sigma^2$(Å$^2$) is the Debye-Waller factor and $R$ is the overall goodness of fit. Uncertainties in CN are ± 1, in $r$ ± 0.02 Å.

## DISCUSSION

### Batch experiments

The results of the uptake experiments fell into two groups. The first (Cu and Cd on both oxides, Cd on pyrite), had substantial uptake of metal from solution at low concentrations (almost complete at the lowest concentrations), but the efficiency of uptake decreased as the metal loading increased. This behavior suggests a process in which a limited range of sites was available on the mineral surface. Those which were most favorable energetically were occupied first, and the occupation of progres-

**TABLE 4.** Summary of EXAFS data fitting for Cd

| Sample | CN and type | $r$ (Å) | $2\sigma^2$ (Å$^2$) | $R$ |
|---|---|---|---|---|
| Goethite | 6 O | 2.26 | 0.017 | 24.1 |
| | 3 Fe | 3.75 | 0.024 | |
| Lepidocrocite | 6 O | 2.28 | 0.018 | 21.9 |
| | 2 Fe | 3.31 | 0.023 | |
| | 1 Fe | 3.77 | 0.015 | |
| Mackinawite | 4 S | 2.52 | 0.005 | 32.2 |
| Pyrite | 6 O | 2.28 | 0.010 | 36.1 |

*Notes:* CN is coordination number, $r$ is interatomic distance, $2\sigma^2$(Å$^2$) is the Debye-Waller factor and $R$ is the overall goodness of fit. Uncertainties in CN are ± 1, in $r$ ± 0.02 Å.

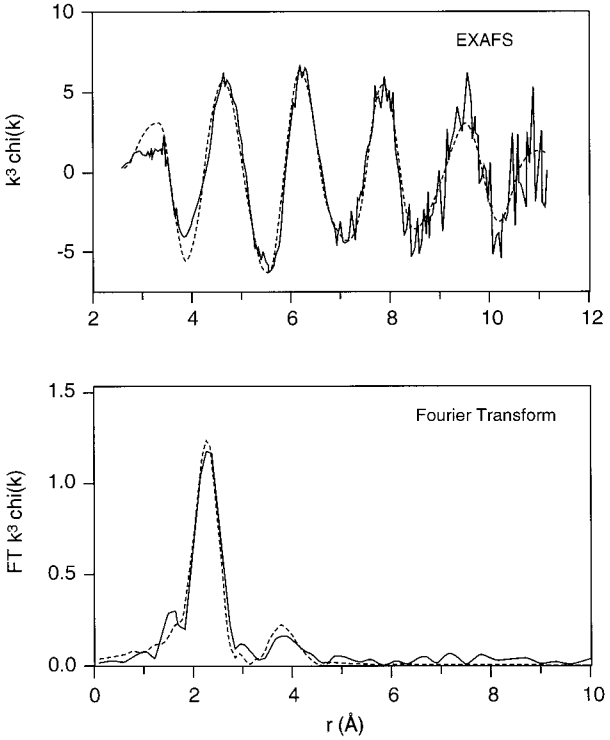


**FIGURE 5.** EXAFS and Fourier transforms for $Cu^{2+}$ on mackinawite (initial solution concentration 1.0 mmol/L; Cu loading 104 mmol/kg).

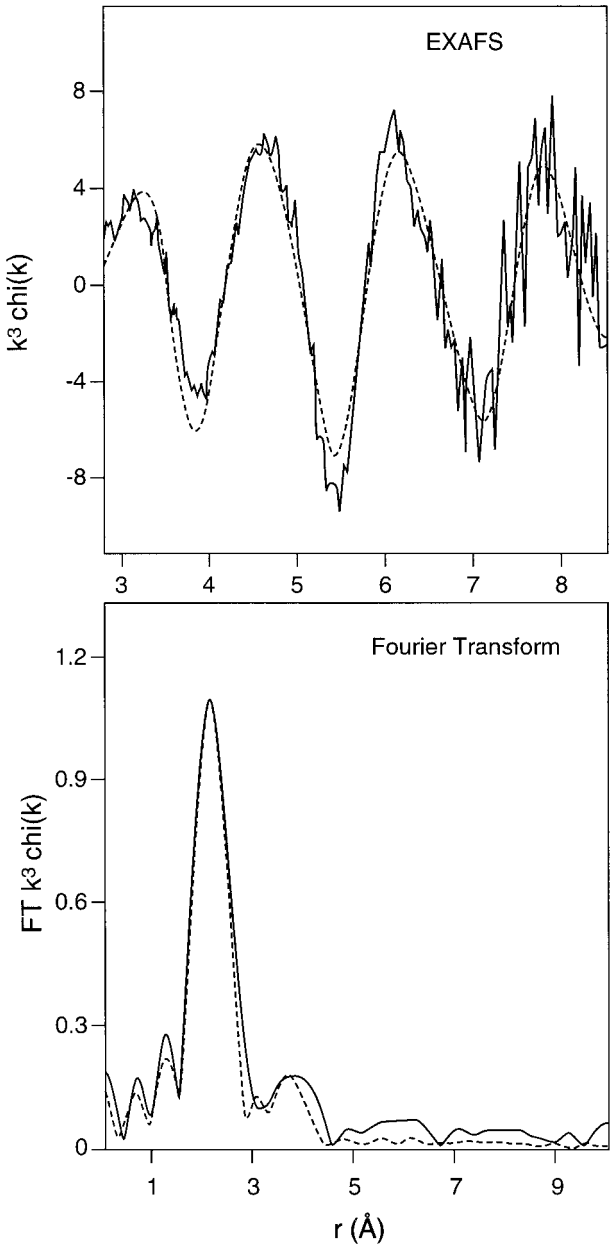


**FIGURE 6.** EXAFS and Fourier transforms for $Cu^{2+}$ on pyrite (initial solution concentration 1.0 mmol/L; Cu loading 102.7 mmol/kg).

sively less favorable sites led to less efficient uptake at higher metal loadings, until eventually the surface was saturated. The two oxide phases reacted differently with Cu and Cd with goethite taking up Cd to a greater extent than Cu, and the opposite occurring on lepidocrocite. This difference suggests that the surface sites were not equally accessible to the two cations. In addition, the capacities of the two different oxides were very different with lepidocrocite having a lower capacity for Cd than goethite but the two minerals' capacities for Cu being approximately equal. The shape of the uptake curve for Cd on pyrite suggests that it reacted with this surface by a similar mechanism to that of metal uptake on the oxide phases, whereas the form of the uptake curve for $Cd^{2+}$ on mackinawite was entirely different, suggesting that the mechanism of interaction is different on the two sulfides.

In the second group (Cu on both sulfides, Cd on mackinawite), uptake at low concentrations was almost quantitative with no decrease in uptake at higher loadings. The uptake curves were also approximately linear with the slopes of the lines similar in all three systems. Uptake was apparently not limited by the availability of sites but rather reflected the growth of a metal-containing phase on the mineral surface, for example, through a precipitation or replacement reaction.

## Geochemical modeling

The results of the model calculations were generally incompatible with the spectroscopic data and illustrated why the results of such equilibrium calculations have to be interpreted with caution. First, the model output was dependent on the reliability and comprehensiveness of the thermodynamic database used. In this case, the database consisted of a wide range of species, including all those that might realistically be expected to form. More importantly in the context of the experiments described here, removal of metal ions from solution by sorption reactions on surfaces was neglected; only reactions leading to precipitation of distinct phases were considered. Third,

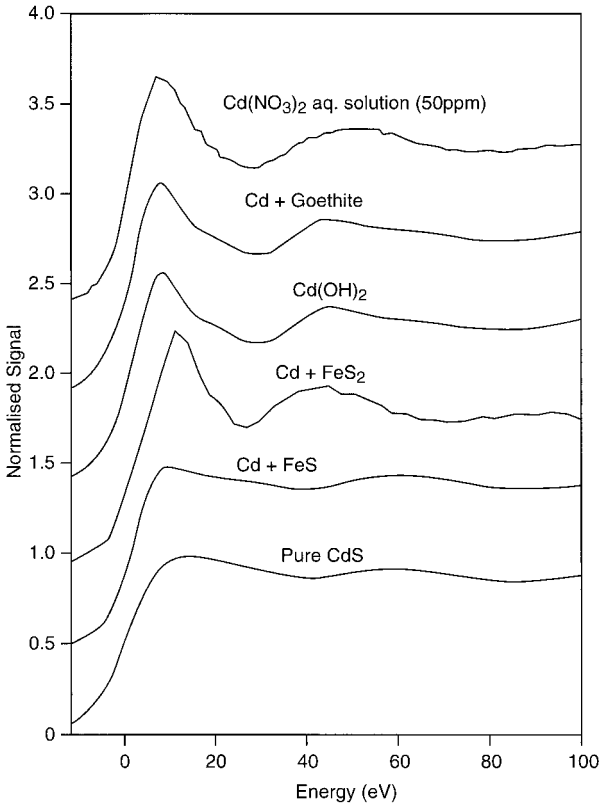


**FIGURE 7.** Cd K-edge XANES for model species and Cd-loaded Fe oxides and sulfides.

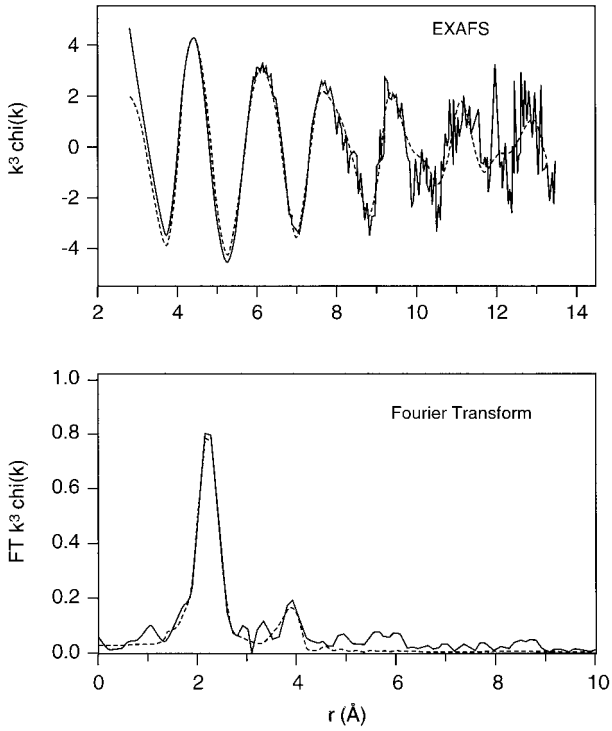


**FIGURE 8.** EXAFS and Fourier transforms for $Cd^{2+}$ on goethite (initial solution concentration 0.4 mmol/L; Cd loading 39.0 mmol/kg).

chemical equilibrium was assumed, which may not have been justified if reactions followed slow kinetics or if attainment of equilibrium was hindered, for example, by formation of coatings on the surfaces of solid phases. Fourth, the thermodynamic data used were determined for pure, crystalline material and it is possible that the substrates used here, particularly the mackinawite, differed in crystallinity and/or purity. Thus, although formation of a distinct phase may be thermodynamically favored, for example, $Cu(OH)_2$ in the Cu experiments, it may not actually occur. For these reasons, we viewed modeling results as useful indicators of the possible course of a reaction rather than a definitive prediction.

### Surface complex formation reactions

In all examples of Cu reaction with oxide surfaces, the first coordination sphere of the $Cu^{2+}$ ion was filled with O atoms in a Jahn-Teller distorted geometry. Although the measured Cu-O distances were different on the two substrates, the differences were not significant within the uncertainty of the EXAFS technique. Cu-metal interactions were identifiable on both substrates, probably demonstrating that a chemical sorption reaction (Bochatay et al. 1997) has occurred, although, as noted above, formation of a distinct $Cu(OH)_2$ phase could not be excluded. Copper and Fe atoms could not be distinguished by XAS but because these interactions are present at all levels of metal loading, this suggests that the interaction was with Fe, in which case the Cu-Fe distances were consistent with ''edge sharing'' (Spadini et al. 1994; Venema et al. 1996) and the additional Cu-metal interaction observed at the highest concentration on lepidocrocite could then represent ''corner sharing'' (Spadini et al. 1994; Venema et al. 1996). It is probable that such corner sharing occurred through the short Cu-O bonds, because this implies a more reasonable Fe-O distance of 1.73 Å in the octahedron. However, it is not possible to exclude formation of Cu polyhedra on the surface, as observed by Farquhar et al. (1997). The Cu-metal distances were similar on the two minerals, reflecting their basic structural similarity. Both consisted of linked, double bands of $FeO_3(OH)_3$ octahedra, linked by corner sharing to form octahedral tunnels in goethite and by edge sharing to give a layered structure in lepidocrocite.

On both oxide substrates, the Cd first shell was essentially the same, and in both cases, second shell interactions with Fe could be identified. Spadini et al. (1994) identified four different linkages of Cd-O octahedra at the surfaces of hydrated ferric oxides, each with a characteristic Cd-Fe distance. On lepidocrocite, we observed a Cd-Fe distance of 3.31 Å, as would be expected for the Cd octahedron sharing an edge with each of two Fe octahedra (Spadini et al. 1994). On both goethite and lepidocrocite, a relatively long Cd-Fe distance around 3.75 Å was also

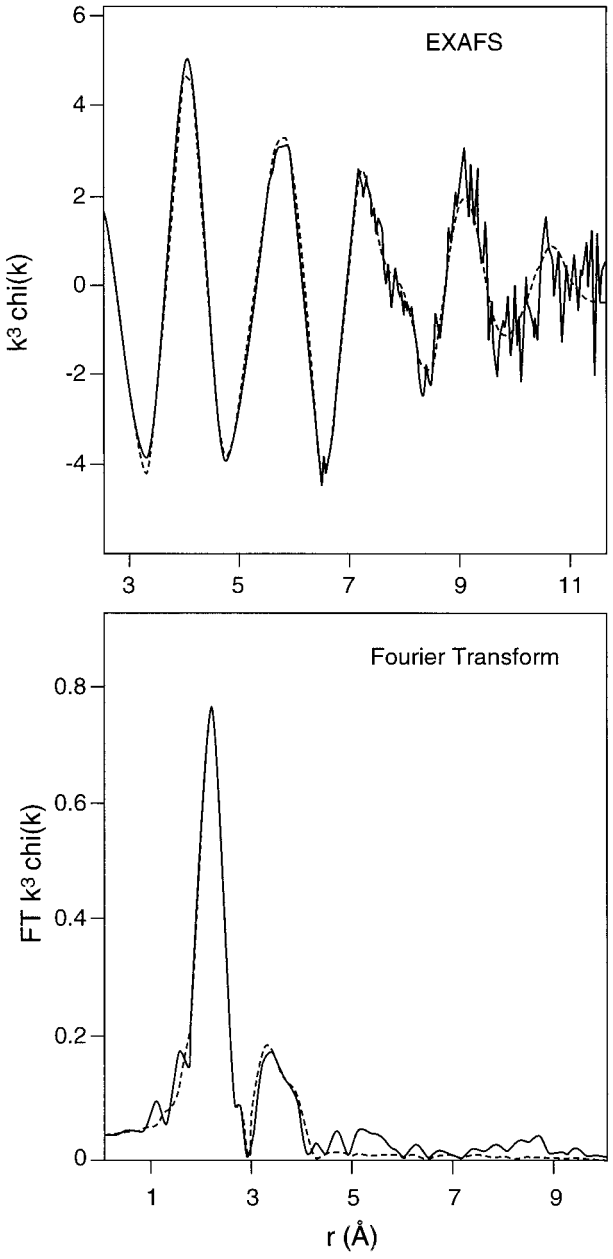


**FIGURE 9.** EXAFS and Fourier transforms for $Cd^{2+}$ on lepidocrocite (initial solution concentration 3.0 mmol/L; Cd loading 36.0 mmol/kg).

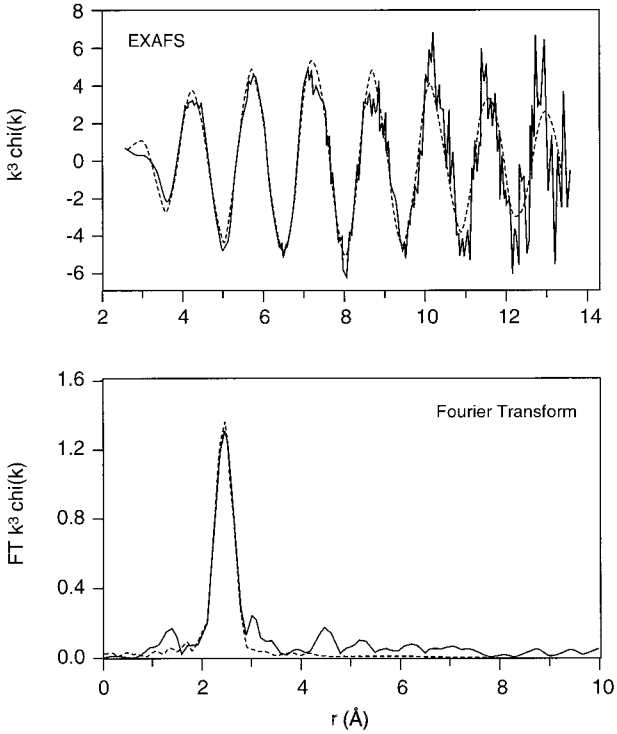


**FIGURE 10.** EXAFS and Fourier transforms for $Cd^{2+}$ on mackinawite (initial solution concentration 5.0 mmol/L; Cd loading 504.6 mmol/kg).

observed, suggesting the fourth of the linkages proposed by Spadini et al. (1994) and involving sharing of just one corner by the Cd and Fe octahedra. Spadini et al. (1994) suggested that the linkages characterized by longer Cd-Fe distances were observed at higher surface loadings of Cd, comparable to those in our experiments. Cd-Fe distances of ~3.5 Å seen in the work of Spadini et al. (1994) were not observed in our experiments. The generally increased Cd-Fe distances, compared to the Cu-metal distances, were consistent with the greater size of the $Cd^{2+}$ ion. Because Cu and Cd could interact with the lepidocrocite surface through both edge and corner sharing, it was not obvious why this mineral should have such different affinities for the two elements but the differences could arise from the greater ''bite'' of the O-Cd-O fragment (3.2 Å) compared with the O-Cu-O fragment (2.7 Å through the ''short'' Cu-O bonds), which could lead to excessive distortion on edge sharing with the surface because the edges of the Fe octahedra were 2.3 Å in length.

Perhaps the most unexpected observation was the behavior of Cd on pyrite, which was completely inconsistent with the thermodynamic calculations. The uptake curve, XANES, and EXAFS all suggested that it reacted with the surface by a different mechanism to Cu and was in approximately octahedral sixfold coordination with O. There are two possible explanations. The Cd could have been taken up as an outer sphere complex, retaining a shell of solvating water molecules. This seems unlikely due to the high capacity and relatively strong binding at low concentrations but is consistent with the absence of any Fe interaction in the EXAFS. Alternatively, the Cd could have formed an inner sphere complex with locally oxidized areas of the pyrite surface. The pyrite was synthesized in a controlled atmosphere and, throughout the experiments, considerable care was taken to exclude air to prevent oxidation, but it is still possible that some oxidation occurred. However, if this was the case, Cu uptake was not comparably affected. Equally, it is difficult to

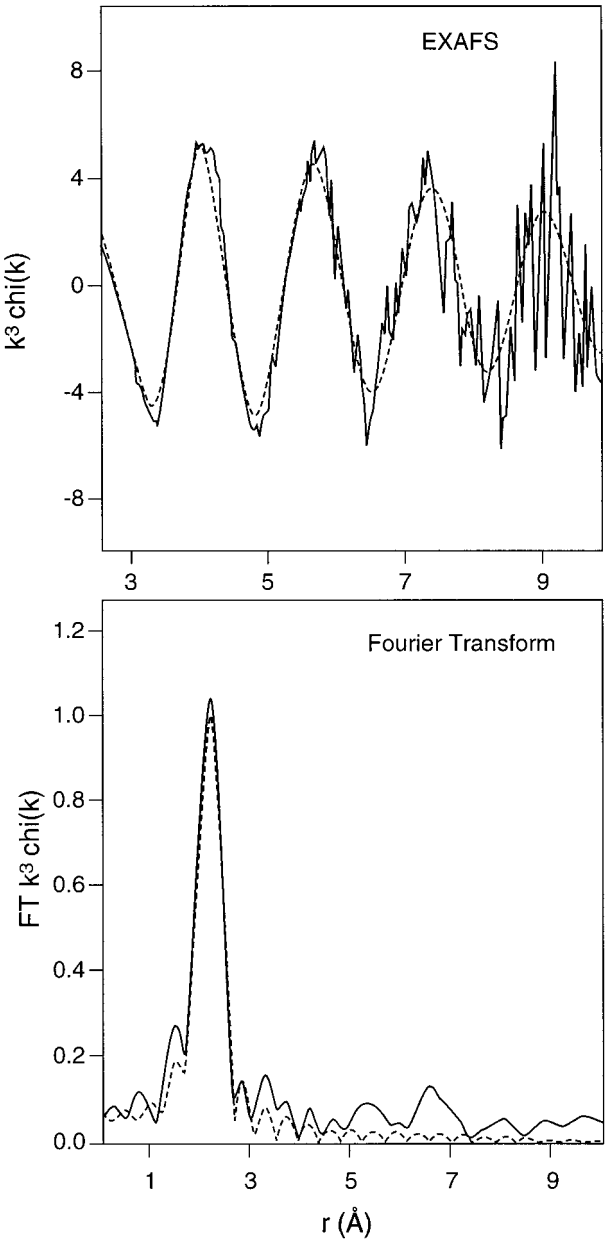


**FIGURE 11.** EXAFS and Fourier transforms for $Cd^{2+}$ on pyrite (initial solution concentration 1.0 mmol/L; Cd loading 80.0 mmol/kg).

envisage that reaction with a degassed aqueous solution of $Cd^{2+}$ would oxidize the surface. Such reactions could account for the complexity of the behavior of Cd reacting with pyrite observed by Kornicker and Morse (1991).

### Surface precipitation/replacement reactions

Two distinct mechanisms are responsible for reactions of this type. An ion in solution can react directly with the mineral surface, altering the local structure and leading to development of a phase of different composition (Parkman et al. 1998). Alternatively, addition of metal ions to a solution may lead to precipitation of a new phase, which, if it is less soluble than the pre-existing mineral, will eventually lead to conversion of the more soluble phase into the less soluble one through a phase transfer process. This second reaction mechanism may be hindered through nucleation of the less soluble phase on the existing particles, leading to overcoating and passivation. XAS cannot distinguish between these reaction mechanisms and can provide only limited information on the extent of reaction but does provide a useful means of identifying the presence of any putative reaction products.

In both the Cu-sulfide systems, XANES and EXAFS analyses showed that well-defined mineral phases formed at all levels of metal loading. On pyrite, the XANES suggested that different sulfide phases (chalcocite and covellite) form depending on the Cu concentration but this could not be confirmed by EXAFS, because the coordination numbers and interatomic distances in these are similar. However, thermodynamic modeling of the reaction of Cu with mackinawite suggests that a hydroxide phase should be formed, yet we found no spectroscopic evidence to support this. The XANES suggested that chalcopyrite formed, and this was consistent with the EXAFS analysis.

The uptake curve for Cd suggested that a discrete phase formed on reaction with mackinawite. XANES demonstrated this clearly, and the coordination numbers and interatomic distances determined from EXAFS were consistent with the formation of a sulfide phase, such as greenockite or hawleyite. Again, thermodynamic calculations did not predict the formation of any solid phases.

## CONCLUSION

The partitioning of metal ions between the solution phase and the surfaces of common minerals is governed by surface processes. Two types of reaction mechanism were identified here: surface complex formation and surface precipitation or replacement reactions. Each reaction type is accompanied by characteristic bulk scale behavior, exemplified by the uptake experiments. Oxide surfaces in general react through surface complex formation, whereas only one example of such a reaction on pyrite was identified. The results of the mineral surface reactions studied here are not in agreement with the thermodynamic modeling, possibly because thermodynamic equilibrium was not completely attained in the experiments. Because large-scale sorption/desorption behavior is strongly dependent on reaction mechanism, it is important to identify the relevant mechanism correctly in the practical application of solution-surface partitioning measurements, such as migration modeling. The outcome of reactions between ions in solution and mineral surfaces depends subtly on the nature of the surfaces, exemplified by the differences in behavior between Cu and Cd on lepidocrocite and on the formation of different Cu sulfide phases, depending on the identity of the sulfide substrate and the concentration of Cu present.

This study also illustrates the complementary nature of the two X-ray absorption spectroscopies used. Whereas EXAFS provides relatively well-defined coordination numbers and interatomic distances, these alone are not always sufficient to distinguish between different reaction products and the XANES provides a useful fingerprint that can define the mineralogy of the reaction product more completely than EXAFS alone. However, the use of XANES only is unwise since the EXAFS provides a second data set with which any mineralogical conclusions must be consistent.

## Acknowledgments

We are grateful to Daresbury Laboratory for the provision of beamtime and to the Natural Environment Research Council (Grant GR3/9690) for financial support.

## References cited

Arthur, D.J.W. and Tyrer, M. (1996) PHREEQE 96 user guide. 77 p. Her Majesty's Inspectorate of Pollution, London..

Balistrieri, L.S. and Murray, J.W. (1982) The adsorption of Cu, Pb, Zn, and Cd on goethite from major ion seawater. Geochimica et Cosmochimica Acta, 46, 1253–1265.

Benjamin, M.M. and Leckie, J.O. (1981) Multiple-site adsorption of Cd, Cu, Zn, and Pb on amorphous iron oxyhydroxide. Journal of Colloid and Interface Science, 79, 209–221.

Binsted, N., Campbell, J.W., Gurman, S.J., and Stephenson, P.C. (1991) SERC Daresbury Laboratory EXCURV92 program. 48 p. Daresbury Laboratory, Warrington.

Bochatay, L., Persson, P., Lövgren, L., and Brown, G.E. Jr. (1997) XAFS study of Cu(II) at the water-goethite (α-FeOOH) interface. Journal de Physique IV, 7 (Colloque C2), 819–820.

DiToro, D.M., Mahony, J.D., Hansen, D.J., and Berry, W.J. (1996) A model of the oxidation of iron and cadmium sulfide in sediments. Environmental Toxicology and Chemistry, 15, 2168–2186.

Dzombak, D.A. and Morel, F.M.M. (1990) Surface Complexation Modeling. Wiley, New York.

Farquhar, M.L., Vaughan, D.J., Hughes, C.R., Charnock, J.M., and England, K.E.R. (1997) Experimental studies of the interaction of aqueous metal cations with mineral substrates: lead, cadmium, and copper with perthitic feldspar, muscovite, and biotite. Geochimica et Cosmochimica Acta, 61, 3051–3064.

Forbes, E.A., Posner, A.M., and Quirk, J.P. (1976) The specific adsorption of divalent Cd, Co, Cu, Pb and Zn on goethite. Journal of Soil Science, 27, 154–166.

Gurman, S.J., Binsted, N., and Ross, I. (1984) A rapid, exact curved-wave theory for EXAFS calculations. Journal of Physics C, 17, 143–151.

Hedin, L. and Lundqvist, S. (1969) Effects of electron-electron and electron-phonon interactions on the one-electron states of solids. Solid State Physics, 23, 1–181.

Joyner, R.W., Martin, K.J. and Meehan, P. (1987) Some applications of statistical tests in analysis of EXAFS and SEXAFS data. Journal of Physics C, Solid State Physics, 20, 4005–4012.

Kooner, Z. (1992) Adsorption of copper onto goethite in aqueous systems. Environmental Geology and Water Science, 20, 205–212.

———(1993) Comparative study of adsorption behavior of copper, lead, and zinc onto goethite in aqueous systems. Environmental Geology, 21, 242–250.

Kornicker, W.A. and Morse, J.W. (1991) Interactions of divalent cations with the surface of pyrite. Geochimica et Cosmochimica Acta, 55, 2159–2171.

Lee, P.A. and Pendry, J.B. (1975) Theory of the extended X-ray absorption fine structure. Physical Review B, 11, 2795–2811.

Lennie, A.R. and Vaughan, D.J. (1996) Spectroscopic studies of iron formation and phase relations at low temperatures. In: Mineral Spectroscopy: A Tribute to Roger G. Burns. Geochemical Society Special Publication, 5, 117–131.

Lennie, A.R., Redfern, S.A.T., Schofield, P.F., and Vaughan, D.J. (1995) Synthesis and Rietveld crystal structure refinement of mackinawite, tetragonal FeS. Mineralogical Magazine, 59, 677–683.

Morse, J.W. and Arakaki, T. (1993) Adsorption and coprecipitation of divalent metals with mackinawite. Geochimica et Cosmochimica Acta, 57, 3635–3640.

Padmanabham, M. (1983) Adsorption-desorption behavior of copper(II) at the goethite-solution interface. Australian Journal of Soil Research, 21, 309–320.

Parkman, R.H., Curtis, C.D., Vaughan, D.J., and Charnock, J.M. (1996) Metal fixation and mobilization in the sediments of the Afon Goch estuary, Dulas Bay, Anglesey. Applied Geochemistry, 11, 203–210.

Parkman, R.H., Charnock, J.M., Livens, F.R., and Vaughan, D.J. (1998) A study of the interaction of strontium ions in aqueous solution with the surfaces of calcite and kaolinite. Geochimica et Cosmochimica Acta, 62, 1481–1492.

Schwertmann, U. and Cornell, R.M. (1991) Iron oxides in the laboratory: preparation and characterization. 137 p. VCH Publishers, New York.

Spadini, L., Manceau, A., Schindler, P.W., and Charlet, L. (1994) Structure and stability of $Cd^{2+}$ surface complexes on ferric oxides. 1. Results from EXAFS spectroscopy. Journal of Colloid and Interface Science, 168, 73–86.

Vaughan, D.J. and Craig, J.R. (1978) Mineral Chemistry of Metal Sulfides. 500 p. Cambridge University Press.

Venema, P., Hiemstra, T., and Van Riemsdijk, W.H. (1996) Multisite adsorption of cadmium on goethite. Journal of Colloid and Interface Science, 183, 515–527.

Watson, J.H.P. and Ellwood, D.C. (1994) Biomagnetic separation and extraction process for heavy metals from solution. Minerals Engineering, 7, 1017–1028.

Watson, J.H.P., Ellwood, D.C., Deng, Q., Mikhalovsky, S., Hayter, C.E., and Evans, J. (1994) Heavy metal adsorption on bacterially produced FeS. Mineral Engineering Conference Proceedings (abstract and paper), Lake Tahoe, Nevada, U.S.A.

Manuscript received May 15, 1998
Manuscript accepted October 15, 1998
Paper handled by Glenn A. Waychunas